Supplement of Nat. Hazards Earth Syst. Sci., 25, 4577–4592, 2025 https://doi.org/10.5194/nhess-25-4577-2025-supplement © Author(s) 2025. CC BY 4.0 License.





# Supplement of

# Drought hazard assessment across Sweden's diverse hydro-climatic regimes

Claudia Canedo Rosso et al.

Correspondence to: Claudia Canedo Rosso (claudia.canedo@kau.se, canedo.clau@gmail.com)

The copyright of individual parts of the supplement might differ from the article licence.

### Sect. S1 Calculation of standardized drought indicators: SPI, SPEI, SSMI, SSI

The standardized drought indicators were defined using the daily simulated precipitation, evapotranspiration, soil moisture, and streamflow from S-HYPE model. The monthly data was defined by the sum of the precipitation and evapotranspiration, and the average soil moisture and streamflow for each month. For the calculation of SPI (see Eq. S1) and SPEI, we used monthly data of precipitation and evapotranspiration applying the SPEI R package: SPEI (Beguería and Vicente Serrano, 2023; Vicente-Serrano et al., 2010). The statistical tests showed that Gamma probability distribution models best the observed precipitation values, aligning with the standard recommendations for calculating SPI in Europe (McKee et al., 1993). The SPEI was defined by computing the monthly difference between precipitation and potential evapotranspiration. And the statistical, distribution used for obtaining the SPEI was the log-logistic distribution, which was considered a suitable distribution based on the findings of Vicente-Serrano et al. (2010). To calculate the Standardized Soil moisture Indicator (SSMI), the SPEI R package and the SPEI function was used, applying the log-logistic distribution (Tian et al., 2021). And for the calculation of Standardized Streamflow Indicator (SSI), applying the SPEI R package and the SPEI function, the log-logistic distribution was used (Teutschbein et al., 2022; Tian et al., 2021).

The standardized drought indicator quantifies anomalies in precipitation, precipitation—evapotranspiration, soil moisture, or streamflow on a dimensionless scale. Monthly values are fitted to a probability distribution (e.g., gamma or log-logistic), and the cumulative probability of each observation is transformed into a standard normal variable with mean 0 and standard deviation 1 (see Eq. (2)). Negative values indicate dry conditions, and positive values indicate wet conditions, allowing comparison across regions and timescales.

Standardized drought indicator = 
$$\frac{X - \mu}{\sigma} = \Phi^{-1}(H(x))$$
 Eq. (2)

where X is the value corresponding to the cumulative probability,  $\mu$  is mean of the standard normal distribution,  $\sigma$  is the standard deviation of the standard normal distribution,  $\Phi^{-1}$  is the inverse of the standard normal cumulative distribution function, H(x) is the cumulative probability from the fitted probability distribution.

## Sect. S2 Spatial-temporal analysis of drought indicators

Figure S1 shows the distribution of the mean SMA values per cluster using a violin plot. Wider sections of the violin indicate a higher probability of SMA values falling within a particular drought severity level. For instance, the largest data density ranges between -1 and 1, indicating predominantly non-drought conditions. However, Clusters C, D, and E showed *extreme* (SMA < -2) and *severe* (SMA from -2 to -1.5) dry periods more frequently. *Moderate* dry periods (SMA from -1.5 to -1) were common across all clusters except cluster A.

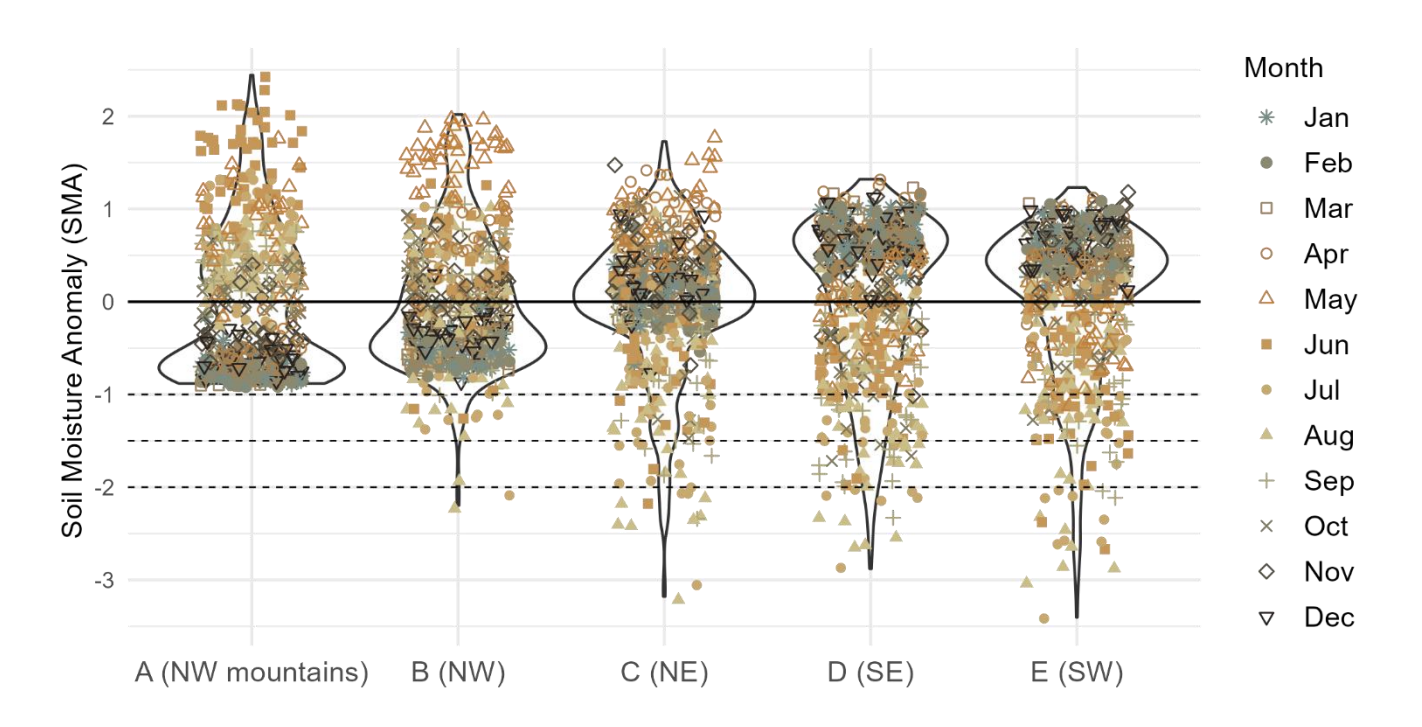


Figure S1. Violin plot of the monthly mean SMA across the 39,635 studied sub-catchments, grouped into the five clusters. Points represent the monthly mean SMA of a sub-catchment. SMA lower than -2 represents extreme drought, SMA values from -2 to -1.5 is severe drought, and SMA from -1.5 to -1 is moderate drought.

#### Sect. S3 Characterization of dry periods in Sweden – Additional material

Figure S2 shows the drought frequency, which represents the total number of dry periods recorded during the study period from 1975 to 2021. In general, short-term meteorological dry periods (including SPI-1, SPI-3, SPEI-1, and SPEI-3) were more frequent and have a lower standard deviation, while short-term agricultural and hydrological dry periods (including SSMI-1, SSMI-3, SSI-1, and SSI-3) were less frequent and showed larger regional variation. The SPEI analysis revealed a high frequency of dry periods during the study period. Specifically, SPEI-1 recorded approximately 70 to 90 dry periods, while SPEI-3 observed around 40 to 50 dry periods (see Fig. S2 left). Long-term dry periods (including SPI-12, SPI-24, SPEI-12, SPEI-24, SSMI-12, SSMI-24, SSI-12, and SSI-24) were less frequent but more uniform across regions. Fewer than 30 dry periods were generally observed across the four standardized indicators for the 12- and 24-month timescales. This corresponds with the progression of drought, as only prolonged precipitation and evapotranspiration deficits result in reduced soil moisture and lower streamflow levels.

The percentage of time in dry conditions due to precipitation deficit (as measured by SPI-1 to SPI-24) ranged from 12 to 18% during the study period (see Fig. S2 right). Drought based on short-term precipitation deficits, often show rapid recovery following precipitation events, which may explain the observed lower percentage of time in dry conditions as measured by SPI-1 and SPI-3. Short-term (SPEI-1 and SPEI-3) and mid-term (SPEI-6) dry periods, as measured by precipitation and evapotranspiration, demonstrated a percentage of time in dry conditions ranging generally from 16% to 20%. The larger percentage of time in dry conditions observed with SPEI compared to SPI highlights the influence of temperature and evapotranspiration, which contribute the persistence of these conditions. The percentage of time in agricultural and hydrological dry conditions (based on soil moisture and streamflow) generally ranged from 14% to 18%. However, parts of southern and northern Sweden experienced from 18% to 30% percentage of time in dry conditions (including SSMI-1 to SSMI-24 and SSI-1 to SSI-24) during the study period. SSMI and SSI reflected the cumulative effects of drought over time and respond to meteorological changes. This could explain the generally lower frequency but longer percentage of time in dry conditions detected by SSMI and SSI.

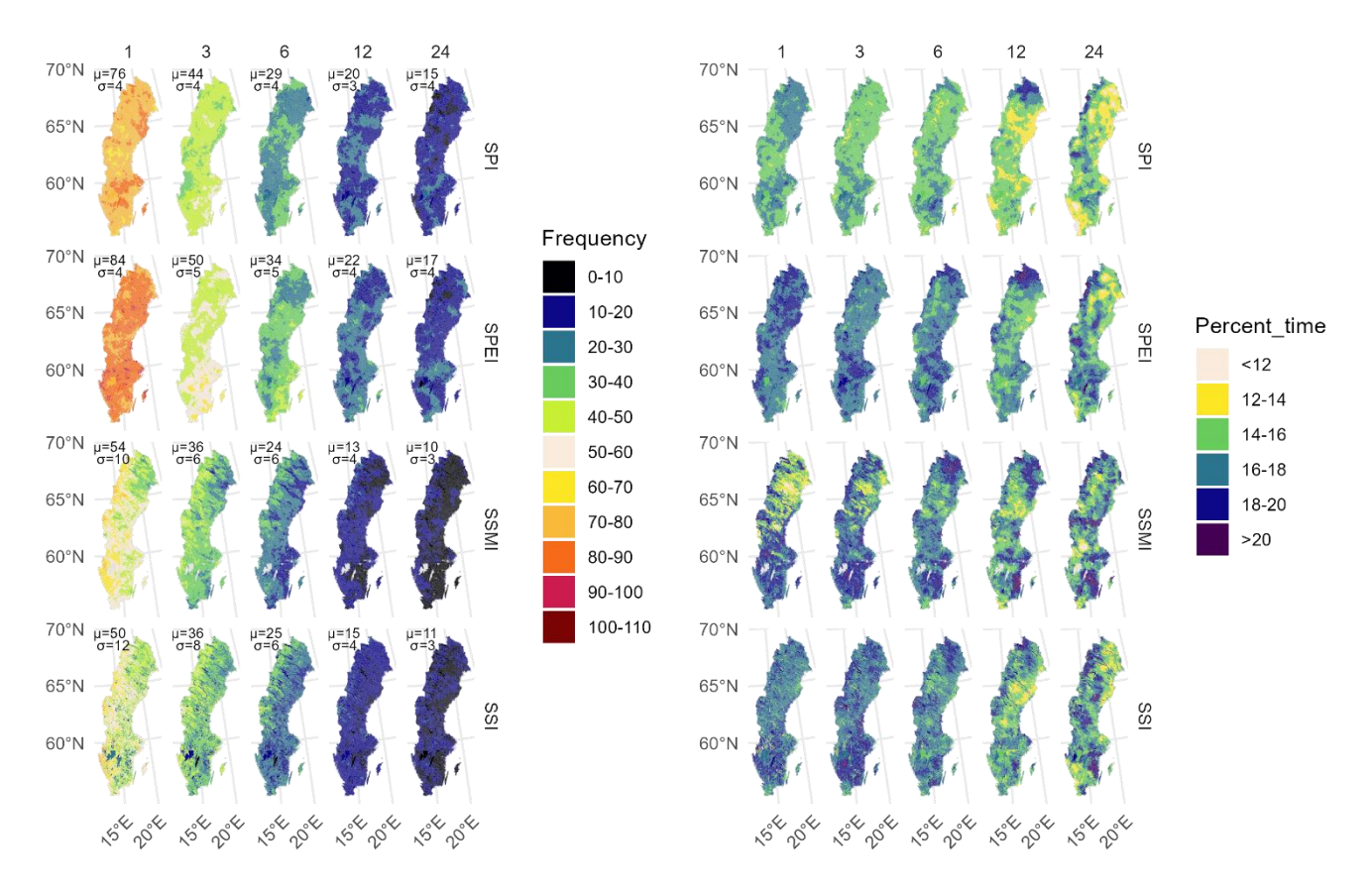


Figure S2. The drought frequency (left) and the percentage of time in dry conditions (right) during the study period 1975 – 2021 for the standardized drought indicators –SPI, SPEI, SSMI, and SSI– for the timescales of 1, 3, 6, 12, and 24 months.

Figure S3 shows the drought intensity for 1976, 1996, and 2018. Largest drought intensity was shown for SPI in 1976 and 1996. Moreover, in 2018, high drought intensity was shown for SPI-1, SPEI-1 and SSMI (1 to 12 months).

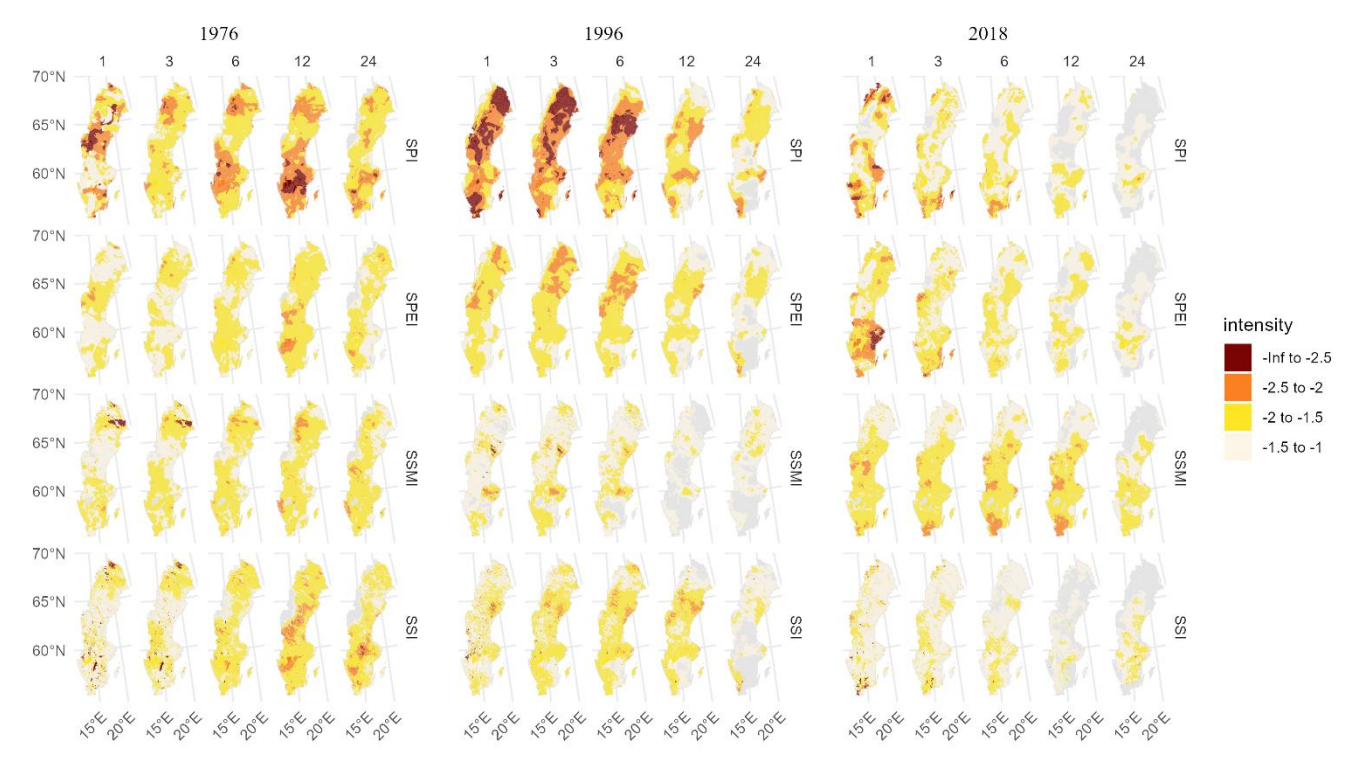


Figure S3. Intensity of the standardized drought indicators –SPI, SPEI, SSMI, and SSI– for the timescales of 1, 3, 6, 12, and 24 months for the years 1976 (left), 1996 (mid), and 2018 (right).

SSMI-1 for cluster A exhibited extreme in over 50% of the catchments during August 2006 and severe dry conditions October 1976, May 1977, July 1980, November 1992, October–November 2002, July 2003, September 2014, and July 2018 (Fig. S4). SSMI-1 for cluster B showed severe dry periods in over 50% of the catchments during April 1985, May 1990, June and November 1992, August 1994, May–June 2002, September-December 2002, July 2003, August 2006, September 2014, and July 2018. SSMI-1 for cluster C showed extreme dry periods in over 50% of the catchments during May 1990, December 2002, January 2003, and July 2018; and severe dry periods in April 1985, October 1989, June 1992, August 1994, May–June 2002, September 2002 – January 2003, August 2006, and June and October 2018. SSMI-1 for cluster D indicated extreme dry periods in June–July 2018; and severe dry periods in August, November–December 1975, February 1977, August 1983, May 1990, June 1992, May 1993, September 2002, June 2008, October 2016, August–December 2018, April 2019 and April 2020 affecting over 50% of the catchments. SSMI-1 for cluster E showed extreme dry periods in June 1992 and April 2019; and severe dry periods in August 1975, July–September 1976, December 1978 – February 1979, January 1982, August 1983, January 1987, May 1990, May 1993, May and July 1994, April 2002, September–October 2002, June 2008, January–February and December 2010, October 2016, June–August 2018, April 2019, and April 2020 affecting over 50% of the catchments.

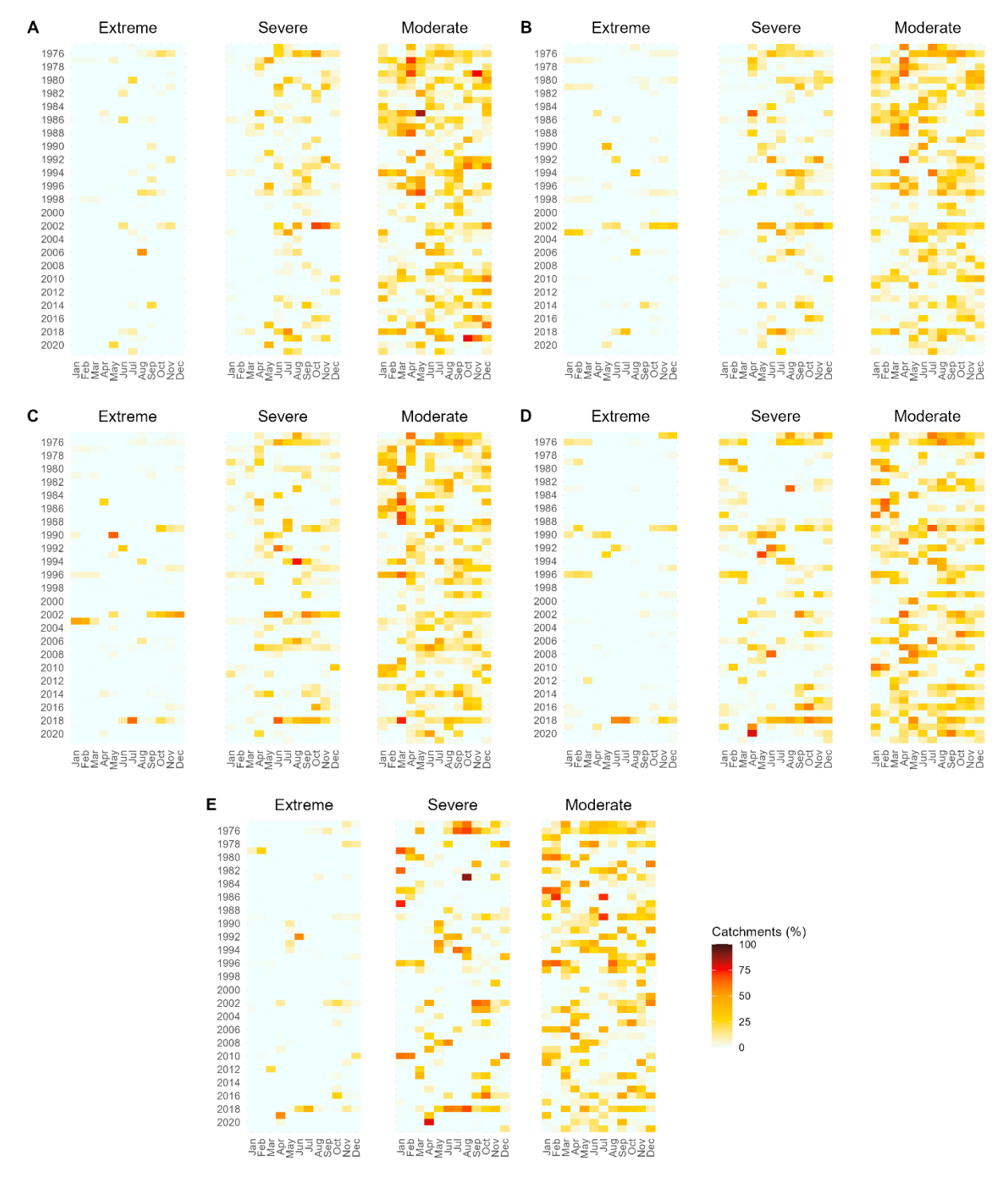


Figure S4. Heatmap of the percentage of catchments in dry conditions for SSMI-1 for cluster A – cluster E by severity level: moderate (-1.5 to -1), severe (-2 to -1.5), extreme  $(\le -2)$ .

### Sect. S4 Trends of dry periods in Sweden

Figure S5 illustrates trends in the severity, intensity, duration and frequency of dry periods across Sweden. Most of the locations show no-significant trends for severity, intensity, or duration. The few significant positive trends in severity and intensity are generally found in parts of northern Sweden, while negative trends in duration generally appear in the northern and western regions. Drought frequency exhibits generally significant negative trends (indicating lower frequency) in parts northern and western Sweden and positive trends in parts of central-eastern and south-eastern Sweden (see Fig. S6). The significant negative trends cover a wider area when assessed using SPEI.

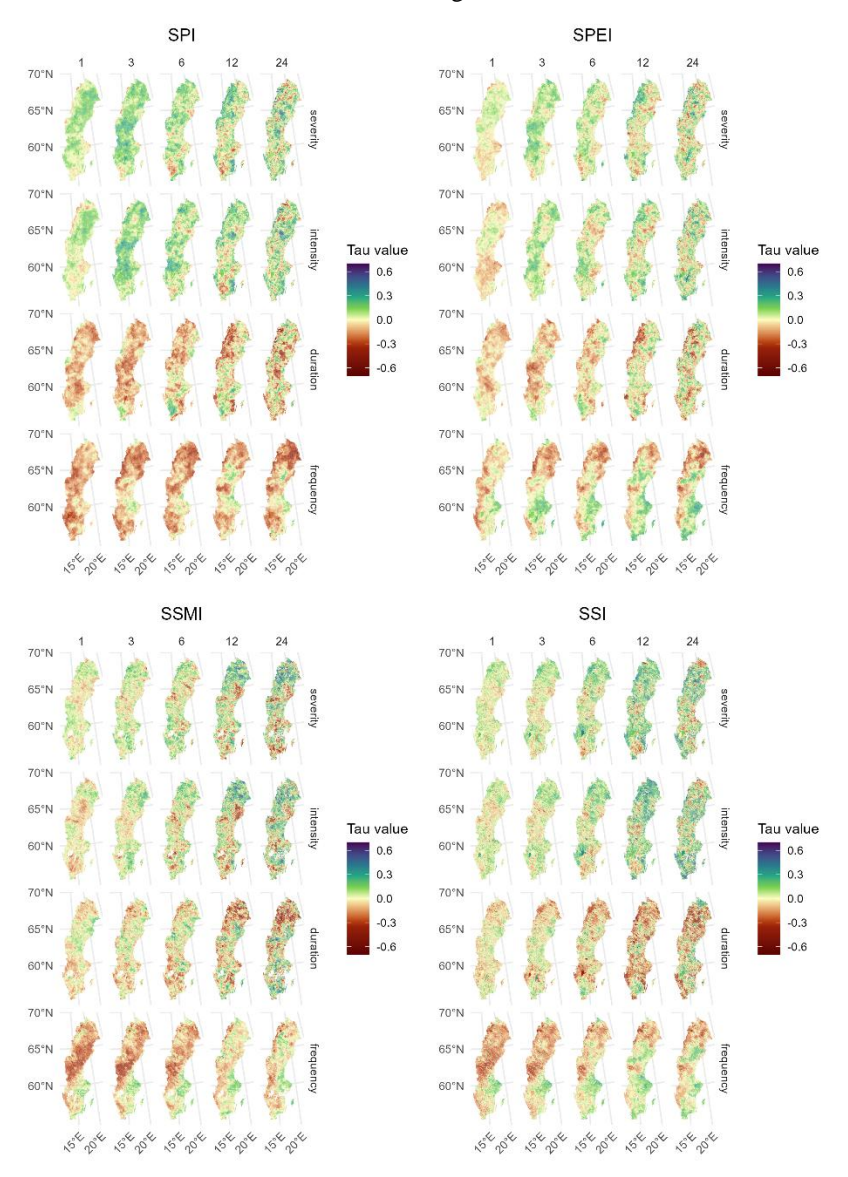


Figure S5. Trends of the dry periods' characteristics computed with the standardized drought indicators –SPI, SPEI, SSMI, and SSI– for the timescales of 1, 3, 6, 12, and 24 months.

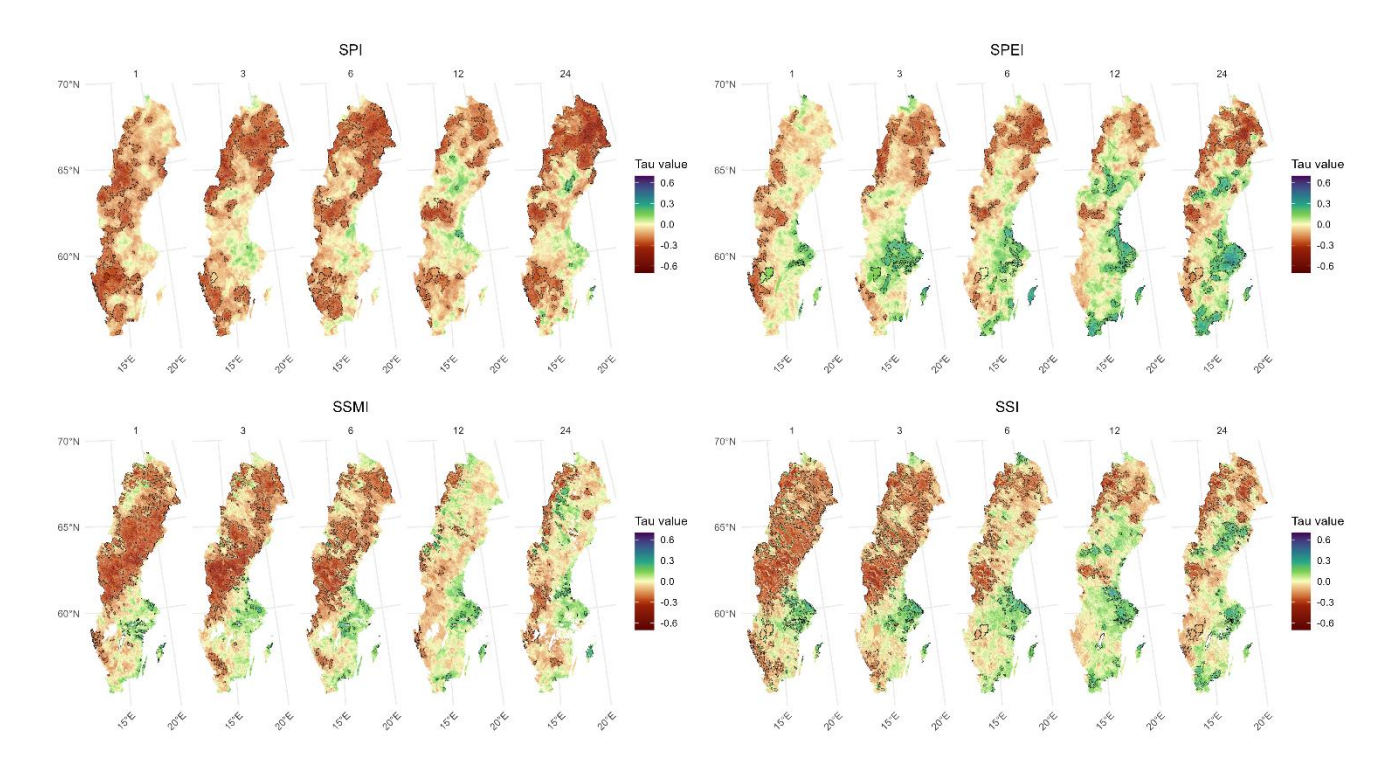


Figure S6. Trends of the dry periods' frequency computed with the standardized drought indicators –SPI, SPEI, SSMI, and SSI–for the timescales of 1, 3, 6, 12, and 24 months. Areas with a black boarder indicate significant tau values (p-value  $\leq$  0.05).